Oil Shale, 2004, Vol. 21, No. 2
pp. 99-114
ISSN 0208-189X

https://doi.org/10.3176/oil.2004.2.02

BEHAVIOR OF ESTONIAN KUKERSITE KEROGEN IN MOLECULAR MECHANICAL FORCE FIELD

Ü. LILLE*

Tallinn Technical University,
Department of Chemistry
15/1 Akadeemia Rd., Tallinn 12618, Estonia

The MM+ force field efficiency in gaining new insights into the structure, properties and genesis of Estonian kukersite kerogen is elucidated. As an initial structure 2D compositional model is used. Based on the ability of kerogen to form hydrogen bonds realistic conformers are designed. The partition of the energy components in various conformers including solvated ones is analyzed. It is shown that the presence of water molecules facilitates the creation of hydrogen bonds i.e. the formation of non-covalent cross-linking. Further experimental and computational research into the swelling behavior of kerogen is promising.

Introduction

Kerogens are insoluble organic components of oil shales, a significant class of alternative fuels, intensively studied by physicochemical methods [1–3]. The results of these studies are often proposed as 2D models representing in a concise way the structural elements of the kerogen, e.g. in [4]. These models, while allowing to draw essential conclusions, do not enable the full interpretation of the obtained information and prediction of the relevant details of kerogen chemical and physical structure.

Molecular modeling using molecular mechanical energy models for description of interatomic and molecular interactions is a powerful tool of the research into the structure and properties of biological and synthetic polymers, zeolites, glasses, etc. [5]. In the field of kerogen and related compound research molecular modeling has been used so far mainly to study certain molecular fragments of kerogen and soluble geomacromolecules as components of coal, bitumens, etc. [6–10].

Inspired by the above-mentioned general success, we tried to use a proper energy model and so to translate the 2D model of Estonian kukersite kerogen (further kerogen) evaluated by ^{13}C MAS NMR spectra [4] into the 3D

* E-mail *lille@chemnet.ee*

language of organic chemistry. The aim of this approach was to gain new insights into the structure and properties of kerogen and to set the tasks for the future experimental research. This article presents the results of the first step towards this goal planned as a longer endeavor of the kerogen modeling.

Some Methodological Aspects

Selection and Short Characterization of MM+ Force Field

In the context of the molecular modeling methodology, amorphous kerogen with low C_{sp^2} and heteroatom content (up to *ca* 25 and 12%, respectively) is in general characterized, similarly to liquids, by short-range order. This is because it does not have any charged species, dipole–dipole interactions varying with interatomic distance r as r^{-3} play insignificant role, and dispersive interactions vary with much higher reverse power. Therefore such molecular solid is amenable to the molecular mechanical (MM) force fields used in organic chemistry [11, 12].

MM+ is an all-atom force field and it is an extension of the latest MM2 version using additional default parameters to widen the range of its use [13]. MM+ uses a set of analytical functions to calculate the changes in the values of bonding and non-bonding energy contributions to the total energy (E_{tot}). The bonding terms are those rising from the bond stretching (bond), angle bending (angle), bond rotation changing the dihedral (torsional) angle, and a cross, stretch-bending term. Van der Waals (VdW) and electrostatic interactions are the non-bonding ones.

Like other force fields, these energy changes are calculated as deviations from the corresponding energies in the idealized standard strain-free molecule which has zero values for all bonded and non-bonded interaction energies between atoms specified into atom types in accordance with their state of hybridization, charge and chemical environment. MM+ uses thirteen carbon, eleven oxygen and eight hydrogen types.

Structural parameters for the standard structures are derived from experimental and quantum-chemically calculated values for the set of smaller molecules in the equilibrium state in the gas phase at zero K temperature. Note that the experimental data on molecules are determined at a finite temperature and are therefore corrected using statistical mechanics formulae [5, p. 273–274; 11, p. 172].

Strategy of Selection of Relevant Conformers

In the light of the classical study of conformational space of cycloheptadecane ($C_{17}H_{34}$) [14] the task of designing conformers of the kerogen seems to be a hopelessly complicated unreasonable task. However, a slightly redeeming feature is the indirectly proved presence of hydrogen bonds in the kerogen [15]. Hopefully one can use these bonds to select realistic conformers i.e. these close to the native ones from their immense number. Therefore we initially study a structural element of 2D kerogen

compositional model, a ketophenol/17 – (3,5-dihydroxy-phenyl)-heptadecan-6-one, with molecular mass 362.6 D, formula $C_{23}H_{38}O_3$, and elemental composition roughly similar to that of kerogen. We try to obtain some understanding of the conformational states of this relatively simple but flexible molecule and to use its ability to form intramolecular hydrogen bond to select corresponding conformers from their obviously large number. Having certain knowledge on the conformational states of this molecule we turn to the model of the kerogen.

Evaluation of the Calculation Results

In this study we focus on the effects of the changes in the structure and molecular environment on the energetics of the system. These changes are generated computationally carrying out geometry optimization (GO) and dynamical simulations in various conditions including the effect of the bulk phase and water. In case one can reasonably interpret the interplay between energy components and structure/environment of the molecular system, the results of the calculations do have certain physical meaning.

Computational Details

HyperChem Release 7 accompanied with an extensive manual is used throughout this work [13]. From a line of force fields available in the HyperChem the MM+ force field mentioned above is chosen.

Data Input

Ketophenol is drawn using HyperChem drawing tool. Model structure of the kerogen is loaded from the corresponding Isis Draw skc file (the removal of two overlaps in the latter results in the slightly modified empirical formula $C_{420}H_{634}O_{44}S_4NCl$, Fig. 1). In accordance with this compositional model, the following atom types (quantities) are treated in the calculations: carbon C4(310), CA(96), C3(6), CO(8), hydrogen H(615), HO(19), oxygen O2(36), O1(8), sulfur S2(2), SA(2), nitrogen N3(1), chlorine CL(1). Carbon atom types in the heterocycles assigned by HyperChem as C3 are assigned manually as CA. Two different approximate initial starting 3D structures are generated rotating the model in the molecular coordinate system.

In general default parameter values of MM+ force field are used, if not shown otherwise.

The following options are used:

- *in vacuo* – electrostatic: bond dipoles, cutoffs none.
- GO: Polak–Ribiere method, gradient 0.09, restraints are used as specified, values of corresponding force constants for the distance K_{fd} (kcal/mol Å^2) and angle K_{fa} (kcal/mol degree^2, see below) are given in shown units. "Restrained" calculations are always followed by single-point calculation excluding energy contributions from the restraints. Periodic boundary conditions (PBC, bulk phase) are used to avoid

boundary effects. Periodic box dimensions are as specified, to account for the effect of water molecules they are added to the box as specified. Outer cutoffs radius equals half of the smallest box size (1/2 *L*, if not specified otherwise).

- Molecular dynamics (MD) options: step size 1 fs (if not specified otherwise), simulation temperature 300 K, heat and cool time 1ps (if not shown otherwise), run time as specified, starting and final temperature 0 K, constant temperature with default bath relaxation constant 0.1 ps (hard coupling), random seed, data collection as specified, restart off, playback and averages are used as specified.
- The options of the Langevin dynamics (LD) accounting for the solvent effects indirectly are those for MD, but step size 0.1 fs is used (longer steps cause abortion), friction coefficient γ as specified.

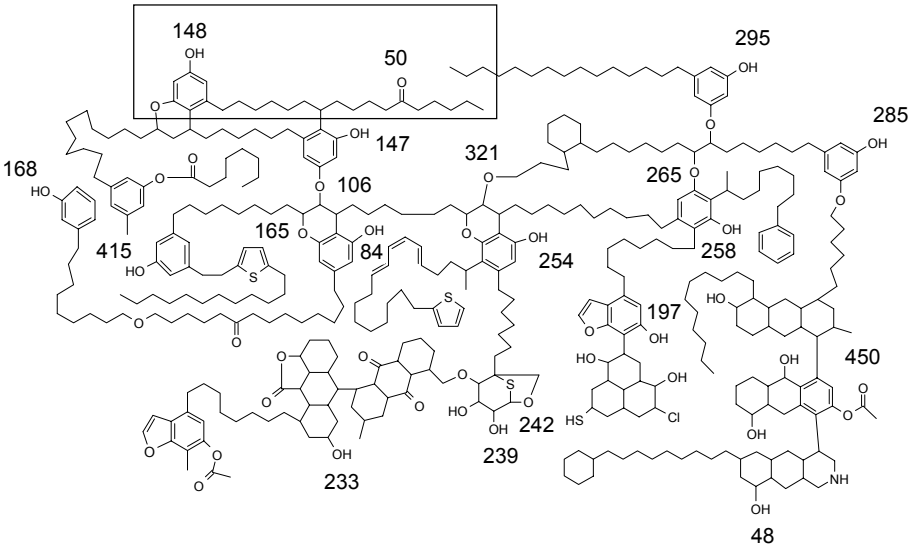

Fig. 1. Compositional 2D model of kerogen. Numbers of twenty relevant oxygen atoms and the structural element used in the initial study are shown

Data Output

Structural measurements are performed using HyperChem tools: the viewers and molecular coordinate systems, the rotations/clip tools. Csv files from MD simulation are plotted using Excel 2000 Program.

Criterion for hydrogen bond creation needs some explanation. HyperChem creates a hydrogen bond if the distance between the donor hydrogen and acceptor atom is less than 3.2 Å, and the angle subtended at the hydrogen by the bonds to the donor and the acceptor (further angle) is greater than 150 degrees. The latter is quite a severe criterion, some investigators use the critical angle value higher than 90 degrees [16]. In the force field used hydrogen bonding interaction is accounted for by a part of

negative component of electrostatic interactions [13]. We note that in general the sign of electrostatic interactions depends on the relative orientation of the dipoles in the space.

Keeping in mind the relevance of VdW interactions in this study, we turn attention to the fact that these interactions comprise two components. These are: positive repulsive close-range exponential component and negative longer-range attractive dispersion $1/r^6$ component (HyperChem does not show these energies separately, therefore the values of VdW interaction energies given below reflect the balance between these two components). Repulsive and attractive forces are exactly balanced at the separation equal to the Lennart–Jones collision diameter (*ca* 3 Å) [5, p. 207].

Results

On the 3D Structure of Ketophenol

Geometry Optimization and MD Simulation

The ketophenol has seventeen rotatable C–C bonds and therefore an enormous number of conformers (*ca* 3^{17}). For our study it is relevant to identify main conformer types of this relatively flexible molecule. The following types are chosen: conformers with fully stretched-out (type 1) or bent side chain (type 2), and cyclic conformer (type 3) where the distance between phenolic proton H59 and carbonylic oxygen O25 (*d*) is less than 3.2 Å (Fig. 2). The distance between these two atoms is used as a characteristic of conformers. In the case of a proper angle value, in the conformer of type 3 there occurs an intramolecular hydrogen bond.

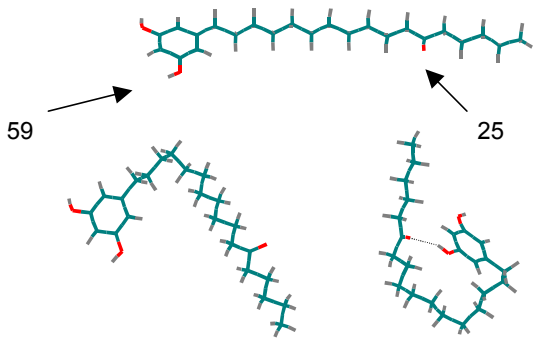

Fig. 2. Ketophenol conformers illustrating the types 1 (top), 2 (bottom, left) and 3 (bottom, right). The latter conformer consists of a hydrogen bond between phenolic polar hydrogen and carbonyl oxygen (atoms No. 59 and 25, respectively). The shown structures are merged selected drafts from HyperChem workspace

Table 1. **Total Energy E_{tot} of the Ketophenol Conformers and Its Components in Vacuum, Bulk and Solvated Bulk Phases, kcal/mol**

Item	Conformer	E_{tot}	Bond	Angle	Dihedral	Van der Waals	Stretch-bending	Electrostatic
Vacuum phase								
1.	(1)	9.02	1.39	3.33	–7.11	11.0	0.308	0.0720
2.	(2)	11.0	1.28	3.93	–4.44	9.89	0.345	0.00983
3.	(3)	9.71	1.28	5.39	–1.31	4.96	0.445	–1.06
4.	(3a)	13.0	1.40	6.22	–3.56	9.94	0.448	–1.56
5.	(3b)	7.84	1.26	4.31	–2.43	6.03	0.390	–1.77
6.	(3c)	7.32	1.32	3.69	–1.38	4.06	0.368	–0.735
Bulk phase								
7.	(1)	8.06	0.758	2.50	–7.13	11.7	0.163	0.0716
8.	(3)	13.5	0.660	4.06	–2.37	12.3	0.198	–1.44
Solvated bulk phase								
9.	(1)	–19.1	1.23	3.00	–5.48	–14.7	0.273	–3.46
10.	(3)	–3.36	0.908	5.81	1.55	–8.13	0.329	–3.83

Computational history:

1 – GO
2 – MD 100 ps, GO
3 – MD 7.6 ps, GO
4 – restraints, GO
5 – restraints, GO, MD 110 ps, GO
6 – restraints, GO, MD 37.7 ps, GO
7 – PBC, box 24.0 × 8.00 × 51.0 Å, GO
8 – PBC, box 22.4 × 8 × 32 Å, GO
9 – PBC, box 20 × 20 × 32 Å, 393 passive water molecules, GO
10 – PBC, box 16.0 × 15.5 × 51.2 Å, 369 passive water molecules, GO

in vacuo

GO of the approximate structure of ketophenol results in the conformer (1) (item *1* in Table 1). In this conformer the side chain is in plane with the phenyl ring, and methylenic hydrogens are all in staggered positions. The phenolic proton closest to carbonylic oxygen is moved from it far away (*d* 17.3 Å). Conformer (1) subjected to a 100-ps MD run at 300 K followed by the GO results in conformer (2) with less favorable torsional interactions and therefore with higher total energy (*d* 10.5 Å, item *2*). Note the slight positive electrostatic interaction energy values in items *1* and *2* showing very weak dipole–dipole interactions caused by the polar carbon–oxygen bonds.

Study of the MD trajectory shows the fluctuations of *d* in the borders *ca* 2.7–19 Å (Fig. 3).

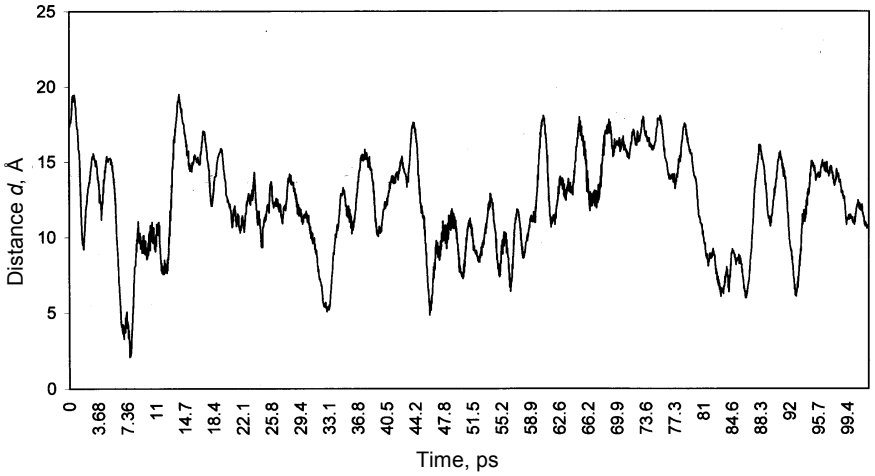

Fig. 3. Fluctuations of distance between phenolic proton H59 and carbonylic oxygen O25 (for *d* values see Fig. 2) during a 100-ps molecular simulation run of ketophenol. Data collection 2 time steps, snapshots period 2 data collection steps

At the same time the angle value varies from *ca* 2 to 160 degrees. As one can estimate from Fig. 3, conformers of type 2 are by far statistically more valid at 300 K than conformer types 1 and 3 (note the result of MD run: see item *2* in Table 1), i.e. the occurrence of the hydrogen bond is possible only in a negligible per cent of the simulation period. A snapshot of such structure at 7.6 ps with minimum *d* value and its subsequent GO results in a cyclic conformer (3) with intramolecular hydrogen bond (*d* 2.68 Å, angle 156 degrees; item *3*). Note that in this conformer the increase in the torsional and angle interaction energy is essentially balanced by the decrease of VdW (and electrostatic) components. Keeping in mind the energetic definition of the hydrogen bond in water by interaction energy minus 2.25 kcal/mol or less [17], the observed hydrogen bond is rather weak.

The cyclic conformer (3a) is easily obtained using restraints (*d* 2.00 Å, K_{fd} 719) and angle 160 degrees (K_{fa} 5.48; item *4*). In obtained conformer (3a)

d and angle values are close to the imposed ones. Increasing the values of the force constants up to 10^5 results in the conformer with *ca* ten-fold higher total energy with slight absolute increase in the negative $E_{el.st}$ value (1.91 kcal/mol, item not shown). As one can suppose, the energy components of conformer (3a) differ from these of conformer (1) prepared *via* restraint-free optimization (item *1*) mainly by the higher angle and torsional strain.

It is clear that a 110-ps MD run (cool time 10 ps, K_{fd} 7, angle not restrained) of the conformer (3a) and a snapshot at 37.7 ps both followed by the GO with the same force constant further lowers the angle and torsional interaction energy (items *5* and *6*, conformers (3b) and (3c)).

In PBC

The smallest box sizes describing the dimensions of the conformers (1) and (3) are 5.6 × 1.8 × 25.7 and 11.0 × 3.63 × 15.9 Å, respectively (the latters vary within some Ångstrom units in different substrate GO calculations) which differ significantly from the cubic box. To avoid artefacts one obviously cannot calculate non-bonded interactions using the 1/2 *L* rule for the cutoffs at these *L* values. However, in the box 24 × 8 × 51.5 Å we still observe the intensity of VdW interactions in the conformer (1) (item *7*) comprising 96.6% of these observed in the calculation without cutoffs (item not shown) and nearly equal to these *in vacuo* (compare items *7* and *1*).

In general, the energy component values calculated for the single molecule *in vacuo* differ rather moderately from these calculated using PBC (compare items *1 vs*. *7* and *4 vs. 8*). This points to the rather slight surface effects on the vacuum/bulk phase boundary and is in accordance with the low density of this bulk phase (0.062 g/cm^3 in the box 24 × 8 × 51.5 Å). Other methods should be used to generate the bulk phase at realistic densities. However, note the trend that more intensive repulsive VdW interactions occur in this special bulk phase compared to these *in vacuo* (items *7* and *8 vs*. *1–6*).

In Solvated Phase

Creating the solvated phase by adding *ca* 370–390 passive equilibrated water molecules to the box results in a rather typical ratio of the water and solute atoms (generally more than ten [18], in our case eighteen). The presence of water molecules affects conformers (1) and (3) in a similar way. The inversion of the sign of VdW interaction energies is of the utmost interest, the repulsion is changed into a strong attraction (items *9 vs*. *7* and *10 vs. 8*). The distance *d* in conformer (1) is 17.9 Å, i.e. by 1.2 Å longer compared to that in the unsolvated bulk phase in the same box dimensions (item not shown). The solvation tries to pull the solute atoms apart. This phenomenon reflects the typical trend in the classical dissolution process and is the manifestation of the general solvent effect modifying the interactions in the solute molecule [19]. Understandably in the solvated phase the contribution of the $E_{el.st}$ to the E_{tot} increases significantly (items *9* and *10*).

Table 2. **Energy Components of Kerogen Model Conformers, kcal/mol**

Item	Conformer/HBP	E_{tot}	Bond	Angle	Dihedral	Van der Waals	Stretch-bending	Electrostatic	Phase, n^*
1.	I/–	532	49.7	269	82.0	116	10.7	3.91	Gas
2.	II/–	371	40.4	193	63.0	61.3	11.1	1.82	Gas
3.	III/–	250	42.5	185	74.7	–65.7	11.3	2.46	Gas
4.	IV/A	210	37.4	184	77.3	–97.5	10.3	–0.736	Gas
5.	V/B	208	37.2	183	77.6	–98.6	10.3	– 1.58	Gas
6.	VI/C	384	42.7	213	179	–56.8	8.18	– 1.98	Gas
7.	VII/D	496	43.8	231	253	–36.7	7.21	– 2.25	Gas
8.	VIII/A	211	37.4	183	77.3	–96.8	10.3	–0.136	Bulk
9.	IX/A	14.2	37.3	187	82.2	–297	10.3	– 5.27	1,697
10.	X/B	11.6	40.9	193	78.6	–308	11.2	– 4.98	1,685
11.	XI/D	447	41.6	210	209	–14.0	6.03	– 6.35	Bulk
12.	XII/D	207	42.0	212	211	–248	6.11	– 15.8	1,534
13.	XIII/D	207	41.9	212	211	–249	6.11	– 15.5	1,777
14.	XIV/D	203	41.9	212	211	–252	6.10	– 15.8	2,031
15.	XV/D	199	42.1	212	211	–257	6.10	– 15.4	3,210
16.	XVI/D	195	42.0	212	211	–261	6.13	–15.6	5,399

* Number of passive water molecules in the periodic box.

Computational history:

1 and *2*– GO
3 and *4* – GO, MD 100 ps, GO
5–*7* – restraints, GO
8–*16* – restraints
8 – PBC, box 3 × 56 Å, GO
9 and *10* – box 3 × 40 Å, GO
11 – MD 12 ps, PBC, box 3 × 56.0 Å, GO
12 – box 38 × 31 × 50 Å, GO
13 – box 39.5 × 32.5 × 51.5 Å
14 – box 41 × 34 × 53 Å, GO
15 – box 50 × 40 × 55 Å, GO
16 – box 3 × 56.0 Å

Simulating the solvent effects in LD conditions, i.e. dragging ketophenol molecule in ketophenol solvent, at low values of γ (1 ps^{-1} and below) the restraint-free conformer (1) transforms into the conformer (2). This is a waited result because as γ approaches zero, the corresponding integration algorithm reduces to the Verlet algorithm used in MD. Using high γ values (up to 10^5 ps^{-1} representing, according to the Stokes law, a rather viscous liquid) the conformer type is retained, the motions of the side chain are essentially damped, and *d* value fluctuates within 0.3 Å. Apparently this conformer enables the best packing of the molecules in the viscous liquid. Less polar ketophenol as a solvent does not affect the solute molecules analogously to the highly polar water, and subsequent GO of LD runs show the energy components close to these *in vacuo* (item not shown).

It follows that the results of calculations of ketophenol energy components reflect in a reasonable way the changes in its structure and molecular environment.

On the 3D Structure of Kerogen

Geometry Optimization and MD Simulation

The kerogen model structure has numerous rotatable C–C bonds and functional groups. The latters comprise 19 polar hydrogen donors (ten phenolic and nine alcoholic hydroxyl groups) and 25 oxygen atoms in ether, ester and carbonyl functions. In principle these donor and acceptor atoms enable to form a significant number of different hydrogen bond pattern (HBP). The calculations limit this enormous quantity to a small number of hydrogen bonds allowed by the energetically reasonable values of structural parameters.

in vacuo

GO of the initial structures results in conformers I and II with spread-out side chains too large to use PBC (box dimensions* are 45.3 × 28.9 × 56.2 and 31.8 × 33.4 × 64.3 Å, respectively, average box volume is 7.1×10^4 $Å^3$) characterized by intensive angle, torsional and repulsive VdW interactions. Conformer I is energetically significantly less favorable (Table 2, items *1* and *2*). Note the positive electrostatic interaction energies in items *1* and *2* (and *3* below) due to the absence of hydrogen bonds.

Optimized structures I and II are subjected to MD simulation at 300 K for 100 ps (100,000 time steps of 1 fs, cool time for structure I 10 ps) followed by GO. As a result, conformers III and IV are obtained (box sizes 23.4 × 19.0 × 42.1 and 32.7 × 23.1 × 34.8 Å, respectively, average volume 2.2×10^4 $Å^3$). Simulation drives the molecular system towards a more compact form (*ca* 3-fold decrease in volume) characterized by attractive dispersive interactions (items *3* and *4* in Table 2). The extremely quick

* Used here for estimation of conformer size.

quench from 300 to *ca* 0 K during 1–10 ps (10^{16}–10^{17} K/s) is similar to a glass-forming process [20].

As estimated from the smallest box dimensions, conformer III has less volume compared to conformer IV, accompanied by more intensive repulsive VdW interactions (keep in mind the balance between interactive and repulsive VdW interaction energies). Further we use conformer IV more favorable energetically and geometrically, i.e. a slight negative electrostatic interaction in the latter points to the hydrogen bond. Indeed, a hydrogen bond is observed between carbonylic oxygen of the ester function (acceptor O450) and a secondary alcohol group (donor O239, *d* H765/O450 2.44 Å, angle 173 degrees), defined as HBP A (item *4* in Table 3).

Table 3. **Hydrogen Bond Pattern of Four Kerogen Model Conformers**

Item	Donor oxygen			Acceptor oxygen		
	No.[*1]	Type	Function	No.	Type	Function
Conformer IV, hydrogen bond pattern A						
1.	239	O2	Alcoholic OH	450	O1	Ester
Conformer V[*2], hydrogen bond pattern B						
2.	48	O2	Alcoholic OH	233	O2	Alcoholic OH
3.	415		Phenolic OH	50	O1	Keto
4.	254			295	O2	Phenolic OH
Conformer VI[*3], hydrogen bond pattern C						
5.	147	O2	Phenolic OH	106	O2	Ether mixed
6.	258			197		Phenolic OH
7.	197			265		Ether mixed
8.	285			242		Ether aliphatic.
Conformer VII[*4], hydrogen bond pattern D						
9.	148	O2	Phenolic OH	197	O2	Phenolic OH
10.	168			165		Ether mixed
11.	84			168		Phenolic OH
12.	295			321		Ether aliphatic

[*1] See Fig. 1; [*2] plus item *1*; [*3] plus items *1–4*; [*4] plus items *1–8*.

A 200-ps MD run at 300 K and 10-ps run at 600 K followed by GO do not add more hydrogen bonds or decrease the volume of conformer (items not shown). Closer study of conformer IV allows to identify three cases including two phenolic hydroxyl groups satisfying the first condition of hydrogen bond formation, i.e. the corresponding bond lengths is less than 3.2 Å. Therefore conformer IV is further subjected to the second GO using four restraints (including the above-mentioned hydrogen bond) for bond length (2 Å, K_{fd} 7,194) and four restraints for bond angles (160 degrees, K_{fa} 4.38) aimed at the insertion of additional hydrogen bonds. As a result, in the obtained conformer V three additional hydrogen bonds are formed (HBP B, item *5* in Table 3) accompanied by the increase in the negative value of

electrostatic interaction energy (item *5* in Table 2). The energy components of the obtained conformer are close to these of the relaxed conformer IV.

Further two subsequent GO runs are performed using additional constraints for remaining eight phenolic hydroxyl groups, i.e. four and four plus four groups (items *6* and *7*, conformers VI and VII in Table 2; HBP C and D, respectively, in Table 3). The hydrogen bond partners are selected within a distance up to 8 Å. To insert these hydrogen bonds, 10-fold default values of corresponding K_f values are necessary. These optimizations result in the understandable large increase in the corresponding interaction energies, i.e. angle, torsional and repulsive VdW and negative electrostatic interactions. Noteworthily, all these minimizations do not affect significantly the dimensions of the smallest box enclosing the kerogen model.

In PBC

Conformers IV and VII enclosed in the boxes with dimensions 3 × 56 Å give rise to conformers VIII and XI, respectively (items *8* and *11* in Table 2). The results of GO are similar to these of ketophenol, i.e. energy component values for conformers V and VIII are rather close. However, conformer XI is favored in comparison to conformer VII by *ca* 50 kcal/mol. It seems that an additional 12-ps MD run of the initial conformer VII (see footnote *11* to Table 2) leads to a better local minimum on the potential energy surface characterized by stronger hydrogen bonds, less intensive angle and torsional strain. The space-filled model of this conformer is visualized in Fig. 4.

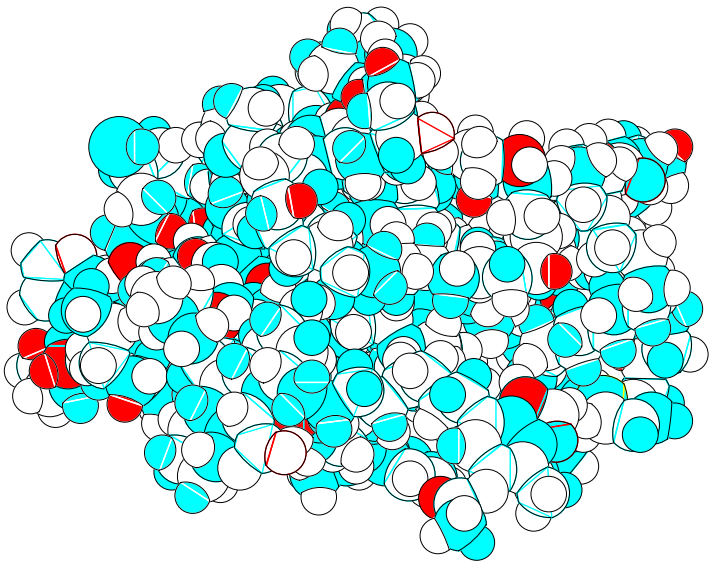

Fig. 4. Kerogen model conformer XI (a picture from the HyperChem workspace, balls rendering mode). Designation of atoms: carbon (smaller sircles) and sulphur (larger circles) – gray, oxygen – black, and hydrogen – white

Noteworthily, in the case of kerogen model the density values of organic material in the bulk phase 0.35–0.41 g/cm^3 are closer to the actual value 1.11 g/cm^3 [21], still too low to enable the calculations of the thermophysical properties of kerogen (e.g. the solubility parameter). In spite of that these calculations point again to the absence of surface effects.

In Solvated Phase

Conformers IV, V, and VII are solvated in the periodic boxes with dimensions enabling the distance between the farthest solute atom to the closest box side more than 7 Å and comprising *ca* 1,500–5,400 water molecules (items *9*, *10*, and *12–16* in Table 2). In this case the ratio of water atoms to this of "solute" is up to 15. Solvation does not change the intensity of the bonding interactions, but the intensity of electrostatic and attractive dispersive interactions increases many times. The increase in electrostatic interaction energy shows the formation of additional hydrogen bonds between solute and water, e.g. in conformer XII between one phenolic hydroxyl group and water molecule. The high intensity of negative VdW interactions is of the most interest. We believe that the increase in $1/r^6$ attractive forces drawing the non-bonded atoms together is the response of the solute molecule to the forces that water molecules exert on it. As a result, the relevant interatomic distances change insignificantly. The solvated conformer XVI is shown in Fig. 5.

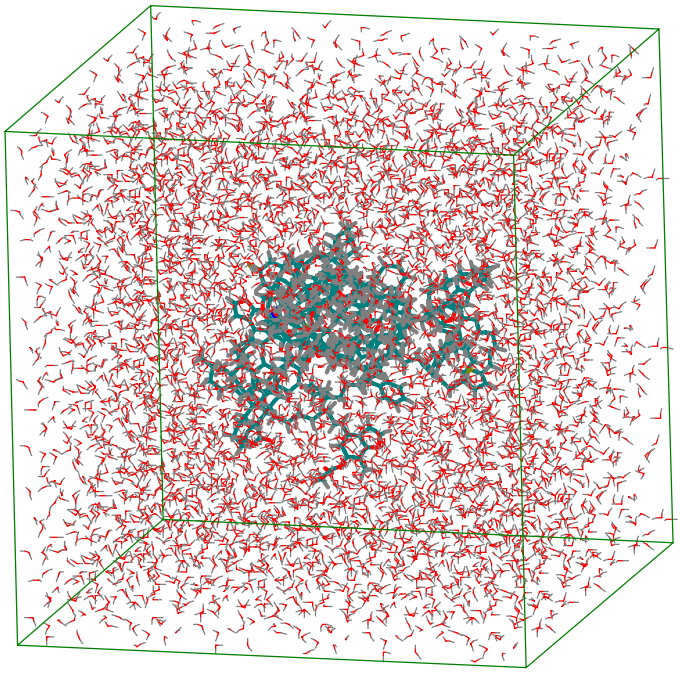

Fig. 5. Solvated kerogen model conformer XVI (see Table 2) with 5,399 water molecules in the periodic box (sticks rendering mode)

LD performed with conformer V ($\gamma = 10^5$ ps^{-1}) does not change significantly its hydrogen bond pattern, no additional hydrogen bonds are formed (item not shown).

The results of the simulations show that the additional angle and torsional strain accompanying the formation of hydrogen bonds in the solvated model kerogen can be balanced at the expense of negative VdW interaction energy appearing as a result of interaction with water molecules. (E_{tot} values of items *2–4 vs* items *9*, *10*, and *12–16* in Table 2). Note the weak dependence of this interaction on the number of water molecules in the box showing roughly close values of solvent accessible surfaces of these conformers. The geochemical significance of the described phenomenon has been treated in another report of the author [22].

It should be pointed out that the locations of the hydrogen bonds designed in this research are not the only possible ones; the model is too flexible to reach unequivocally the best conformers. The main result of the presented calculations is an example on the presence of hydrogen bonds in the kerogen and the elucidation of the role of water in their formation.

In the future research the computational programs enabling to reach real densities of organic material in the calculation box should be used. The experimental and computational study of the interactions of kerogen with organic solvents and the simulation of its swelling behavior is very promising.

Conclusions

Observing the behavior of the kerogen compositional model in the MM+ force field allows generating kerogen conformers with various hydrogen-bonding pattern. In the case of the most intensive hydrogen bonding, all phenolic hydroxyl groups are fixed in these bonds. Creating of hydrogen bonds is accompanied by an essential increase in angle and torsional interactions energies. In the presence of water molecules these additional interaction energies are balanced by the attractive dispersive forces appearing as a result of forces exerted by the water molecules on the kerogen.

Acknowledgements

The author is grateful to Dr. O. Parve, Prof. J. Soone and Estonian Science Foundation for financial support (Grant No. 5624), and to Dr. A. Metsala and Prof. T. Pehk for customizing the computational programs.

REFERENCES

1. *Whelan, J.K., Thompson-Rizer, C.L.* Chemical methods for assessing kerogen and protokerogen types and maturity // Organic Geochemistry. Principles and Applications / M.H. Engel and S.H. Macko (eds.). – New York, London : Plenum Press, 1993. P. 289–353.
2. *Larter, S.R., Horsfield, B.* Determination of structural components of kerogens by the use of analytical pyrolysis methods // *Ibid.* P. 271–288.
3. *Senftle, J.T., Landis, C.R., McLaughlin, R.L.* Organic petrographic approach to kerogen characterization // *Ibid.* P. 355–374.
4. *Lille, Ü., Heinmaa, I., Pehk, T.* Molecular model of Estonian kukersite kerogen as evaluated by ^{13}C MAS NMR spectroscopy // Fuel. 2003. Vol. 82, No. 7. P. 799–804.
5. *Leach, A.R.* Moolecular Modeling. Principles and Applications. – Harlow, England Pearson Education, 2001.
6. *Cody, G.D., Saghi-Szabo, G.* Calculation of the ^{13}C NMR chemical shift of ether linkages in lignin-derived geopolymers: Constraints on the preservation of lignin primary structure with diagenesis // Geochim. Cosmochim. Acta. 1999. Vol. 63, No. 2. P. 193–205.
7. *Kubicki, J.* Models of natural organic matter and interactions with organic contaminants // Org. Geochem. 1999. Vol. 30, No. 8. P. 911–927.
8. *Nomura, M., Artok, L., Murata, S., Yamamoto, A., Hama, A., Gao, H., Kidena, K.* Structural evalution of Zao Zhuang coal // Energy & Fuels. 1998. Vol. 12, No. 4. P. 512–523.
9. *Murgich, J., Abanero, J.A., Strausz, O.P.* Molecular recognition in aggregates formed by asphaltene and resin molecules from the Athabasca oil sand // *Ibid.* 1999. Vol. 13, No. 3. P. 278–286.
10. *Zhao, S., Kotlyar, L.S., Woods J.R., Sparks B.D., Gao, J., Kung, J., Chung, K.H.* A benchmark assessment of residues: comparison of Athabasca bitumen with conventional and heavy crudes // Fuel. 2002. Vol. 81, No. 6. P. 737–746.
11. *Burkert, U., Allinger, N.L.* Molecular Mechanics. – Washington, D.C. : American Chemical Society, 1982.
12. *Sun, H.* Compass: An *ab initio* force-field optimised for condensed-phase applications. Overview with details on alkane and benzene compounds // J. Phys. Chem. B. 1998. Vol. 102, No. 11. P. 7338–7364.
13. HyperChem. – Hypercube Inc., 2002.
14. *Saunders, M., Houk, K.N., Wu, Y.D., Still, C., Lipton, M., Chang, G., Guida, W.C.* Conformations of cycloheptadecane. A comparison of methods for conformational searching // J. Am. Chem. Soc. 1990. Vol. 112, No. 5. P. 1419–1427.
15. *Lille, Ü., Heinmaa, I., Pehk, T.* Investigation into kukersite structure using NMR and oxydative cleavage methods: On the nature of phenolic precursors in the kerogen of Estonian kukersite // Oil Shale. 2002. Vol. 19, No. 2. P. 101–116.
16. *Gestoso, P., Brisson, J.* Effect of hydrogen bonds on the amorphous phase of a polymer as determined by atomistic molecular modeling // Computational and Theoretical Polymer Science. 2001. Vol. 11, No. 4. P. 263–271.

17. *Jorgensen, W.L., Chandrasekhar, J., Madura, J.D*. Comparison of simple potential functions for simulating liquid water // J. Chem. Phys. 1983. Vol. 79, No. 22. P. 926–935.
18. *Yun-Yu, S., Lu, W., Van Gunsteren, W.F*. On the approximation of the solvent effects on the conformation and dynamics of cyclosporin A by stochastic dynamics simulation techniques // Molecular Simulation. 1988. Vol. 1, No. 3. P. 369–383.
19. *Rigby, M., Smith, E.B., Wakeham, M.A., Maitland, G.C*. The Forces Between Molecules. – Oxford : Clarendon Press, 1986. P. 192–195.
20. *Schober, H.R.* Molecular dynamics in amorphous solids and liquids // AIP Conf. Proc. Melville, New York: American Institute of Physics,1999. P. 191–202.
21. Handbook of Oil Shale Refiner. – Leningrad : *Khimiya*, 1988. P. 34.
22. *Lille, Ü.* Effect of water on the hydrogen bond formation in Estonian kukersite kerogen as revealed by molecular modeling // Fuel. 2004. Vol. 83, No. 9. P. 1267–1268.

Presented by A. Raukas
Received December 8, 2003